The Canadian Mineralogist
Vol. 34, pp. 469-478 (1996)

PHLOGOPITE CRYSTALLIZATION IN CARBONATITIC MAGMAS FROM UGANDA

GEORGE R. McCORMICK

Department of Geology, The University of Iowa, Iowa City, Iowa 52242, U.S.A.

MICHAEL J. LE BAS

Department of Geology, The University of Leicester, Leicester LE1 7RH, U.K.

Abstract

We have determined the composition of zoned phlogopitic mica from two carbonatite complexes in Uganda by electron-microprobe analysis, and compared our findings with results for carbonatites in Arkansas and the Transvaal. The mica phenocrysts and xenocrysts, as well as calcite-cotectic phlogopite, are good indicators of the evolving chemistry of the carbonatitic magma and fenitizing fluids. Early-crystallizing phlogopite commonly shows evidence of decreasing Fe/(Mg + Fe) value, reflecting incipient precipitation of magnetite as the Fe^{3+}/Fe^{2+} ratio rises in the magma. The level of Al decreases in the mica owing to its low availability in the carbonatitic magma, which drives the mica composition toward "ferriphlogopite". Cessation of magnetite precipitation allows the "ferriphlogopite" to zone toward "ferribiotite". At this stage, crystallization of mica ceases, only to be renewed in some complexes when wallrock assimilation adds Al, alkalis and Si to the magma. This high-Al phlogopite incorporates Ba. Micas in individual complexes show properties peculiar to that complex, but the general indications are that the availability of Al and the ratio Fe^{3+}/Fe^{2+} in the carbonatitic magma are the main factors governing the composition of the phlogopitic mica.

Keywords: phlogopite, "ferriphlogopite", carbonatite, Busumbu, Sukulu, Uganda.

Sommaire

D'après les données sur la zonation du mica phlogopitique provenant de deux massifs de carbonatite de l'Ouganda (Busumbu et Sukulu), et de carbonatites de l'Arkansas et du Transvaal, la composition des phénocristaux et xénocristaux, de même que de la phlogopite en relation cotectique avec la calcite, s'avère un bon indicateur de l'évolution de la composition du magma carbonatitique et des fluides responsables de la fénitisation associée. La phlogopite précoce montre assez couramment une diminution du rapport Fe/(Mg + Fe) à cause du début de cristallisation de la magnétite, qui accompagne l'augmentation du rapport Fe^{3+}/Fe^{2+} dans le magma. La quantité d'aluminium dans le mica diminue à cause de sa rareté dans le magma carbonatitique, ce qui pousse la composition du mica vers le pôle "ferriphlogopite". La cessation de la précipitation de la magnétite mène ensuite à une zonation vers le pôle "ferribiotite". A ce stade, la cristallisation du mica cesse, pour recommencer plus tard dans le cas de certains complexes suite à l'assimilation des roches encaissantes, ce qui fournit Al, les alcalins et Si au magma. Cette phlogopite alumineuse peut incorporer le Ba. Les micas de complexes intrusifs particuliers ont des caractéristiques propres au complexe, mais en général, la disponibilité de l'aluminium et le rapport Fe^{3+}/Fe^{2+} dans le magma constituent les facteurs importants régissant la composition du mica phlogopitique.

(Traduit par la Rédaction)

Mots-clés: phlogopite, "ferriphlogopite", carbonatite, Busumbu, Sukulu, Ouganda.

Introduction

Color zoning in biotite and phlogopite commonly observed in carbonatites is usually attributed to the evolving chemistry of the host carbonatitic magma (Gaspar & Wyllie 1987, McCormick & Heathcote 1987, Le Bas & Srivastava 1989). Phlogopitic mica is a common constituent of coarse-grained calcio-carbonatites and is less common in fine-grained calciocarbonatites; mica is rarely present in ferro-carbonatites, and where present, is biotitic. The variation in composition cannot be ascribed simply to changing P–T conditions, as phlogopite has a wide range of stability from mantle conditions (Modreski & Boettcher 1973) to subvolcanic settings (Woolley 1969).

This study began as a detailed electron-microprobe examination of the zoning in phlogopite of the Busumbu and Sukulu carbonatite complexes of eastern Uganda. The path of crystallization determined from

the composition of all zones in a well-zoned xenocryst of mica from the Busumbu carbonatite is similar to portions of those paths of crystallization described for the Arkansas carbonatites (McCormick & Heathcote 1987, Heathcote & McCormick 1989) and to that found in the Nooitgedacht complex in Transvaal, South Africa (Clarke *et al.* 1993). Since the data come from such widely spaced localities, such processes may be common to all carbonatites.

The detailed study of phlogopite crystals, results of which are presented here, involved many tens of electron-microprobe analyses from core to rim. The compositional variation can be partly correlated with the changing availability of Al in the host carbonatitic magma. These changes seem related to fractional crystallization and to contamination by interaction with fenitized wallrock.

Carbonatite Complexes

Uganda

The Busumbu bodies of carbonatite studied lie on the western side of the Bukusu alkaline ring complex in eastern Uganda, located 50 km southwest of Mt. Elgon, near the Kenya – Uganda border. It is mid-Tertiary in age, 6 km in diameter, and surrounded by an aureole of potassic fenite 1–2 km wide (Baldock 1973). Carbonatite forms discontinuous outcrops of inwardly inclined sheets emplaced in pyroxenite and ijolite; about 20 boreholes penetrate the complex (Baldock 1967, 1973). Four fresh samples of calciocarbonatite [P5(36,37,38,39)] were taken from borehole no. 13 at depths of 21.6, 23.5, 23.8 and 32.3 m below the surface, respectively. The drill core as a whole shows relics of pyroxenite and ijolite as strips of xenoliths in banded white coarse-grained calciocarbonatite, the bands consisting of primary mica and magnetite. Commonly, the pyroxenite is fragmented and fenitized by fluids related to the white carbonatite. The mica, which is present as clots and along cracks in the white carbonatite, is of the same composition as that which rims the pyroxenite xenoliths.

Sukulu is a mid-Tertiary complex 4 km in diameter near Tororo, approximately 80 km southwest of Mt. Elgon. At the surface, it is composed entirely of carbonatite, mainly coarse-grained calciocarbonatite (Davies 1956, King *et al.* 1972), but in the boreholes there are rare and small relics of pyroxenite and amphibole–mica rock and bands and clots of mica and apatite. Six fresh samples of calciocarbonatite were taken [P4(45,46)] from borehole 1 on hill C at depths of 24.4 and 25.9 m, samples [P4(73,74,75)] from borehole 2 on hill C at depths of 24.1, 24.4 and 31.4 m, and sample [P4(346)] from borehole 1 between hills A and B at a depth of 27.4 m. All consist of calciocarbonatite with brown mica, [green in P4(74)], and some apatite and magnetite.

South Africa

The Nooitgedacht plutonic carbonatite complex is situated adjacent to the Kruidfontein carbonatite caldera complex in the Transvaal, recently described by Clarke *et al.* (1993); both are Proterozoic. Nooitgedacht comprises a calciocarbonatite intrusion about 2 km in diameter surrounded by syenite and fenite (Verwoerd 1967).

Calciocarbonatite

Only samples of calciocarbonatite are considered here; thus the Mg/Fe variations in the mica cannot be ascribed to the presence of magnesiocarbonatite or ferrocarbonatite. In these samples of calciocarbonatite, mica, pyroxene and amphibole are present in xenoliths and as xenocrysts (mineral grains exhibiting one or more episodes of resorption and overgrowth).

Busumbu, Uganda

The analyzed samples of phlogopite-bearing carbonatite at Busumbu are typical calciocarbonatite with twinned crystals of calcite exhibiting triple junctions. Samples [P5(36,37,39)] are coarse-grained calciocarbonatite with xenoliths of apatite pyroxenite [ijolite in P5(39)]. Between the calciocarbonatite and pyroxenite is a zone of brown euhedral flakes of mica which compositionally lie on the biotite – phlogopite boundary (taken to be at Mg:Fe = 2:1). The mica flakes show normal pleochroism with X orange brown and $Y = Z$ brown; some have a darker orange rim.

Sample [P5(38)] from Busumbu consists of a phlogopite–apatite calciocarbonatite with rare needles of blue-green amphibole. The apatite occurs in clusters of rounded crystals. The phlogopite occurs as individual grains as well as xenocrysts and clusters of grains.

The phlogopite crystals in the calciocarbonatite are pleochroic (X pale yellow green, $Y = Z$ pale brown) showing a resorbed margin and undulose extinction. One crystal shows a relict core of darker mica from an earlier period of crystallization; all grains have a narrow orange rim with normal pleochroism (Fig. 1). The phlogopite around melteigitic xenoliths and in fractures in the xenoliths is more strongly deformed than that in the calciocarbonatite and has normal pleochroism (X yellow-green, $Y = Z$ red-brown).

Sukulu, Uganda

The six samples of calciocarbonatite [P4(45,46,73,74,75,346)] analyzed from the Sukulu complex consist of apatite – magnetite – phlogopite calciocarbonatite, some with trains of bundles of minute fibers of amphibole embedded in the calcite. Small (<0.5 mm) octahedra of pyrochlore and some

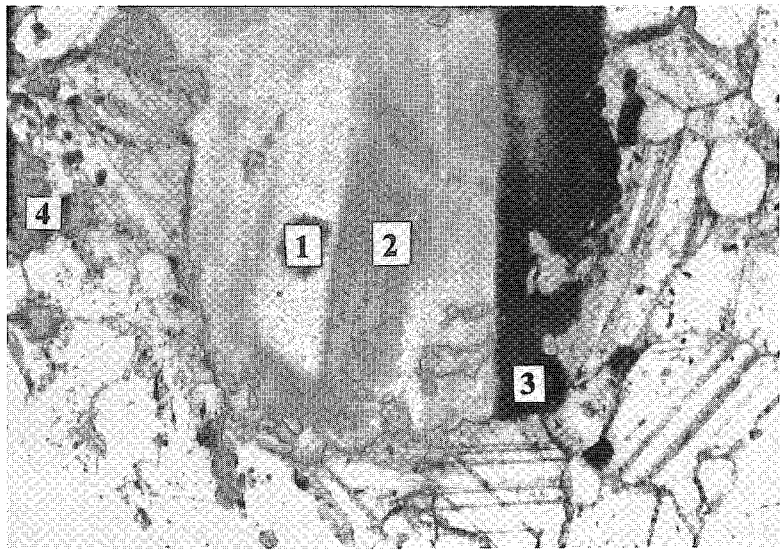

FIG. 1. Zoned crystal of phlogopite in apatite calciocarbonatite from Busumbu (sample BM–1990–P5(38). The larger flake has a parallelogram-shaped green-gray relict core, is pale brown in the greater part of the crystal, and is zoned to darker brown toward the edge, with a ragged and resorbed rim. Field of view is 5 mm across. Numbers correspond to the numbers on Figures 4 and 5.

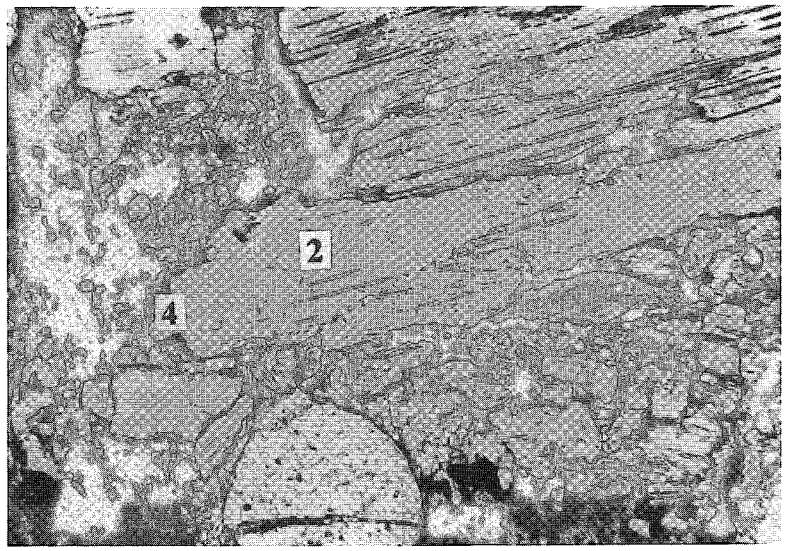

FIG. 2. Zoned, ragged flakes of phlogopite in calciocarbonatite from Sukulu showing evidence of reaction. Core of each relict area of mica is pale green, is abruptly zoned to pale orange along edges and along cracks, and shows an orange-brown reversely zoned pleochroic rim. In the area of small crystals on the left are several small flakes of deeper orange-brown "ferriphlogopite", together with magnetite granules. Field of view is 5 mm across; crossed polars; sample BM–1990–P4(73). Numbers refer to compositional zones described in Fig. 6.

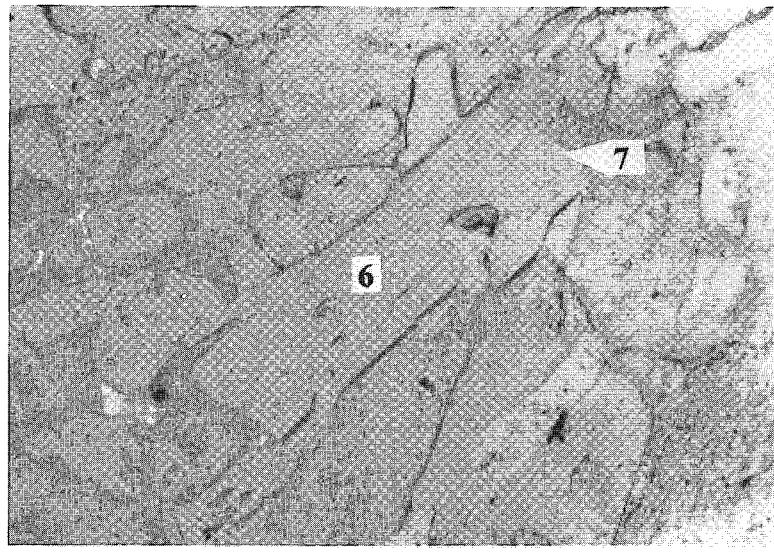

FIG. 3. Undeformed euhedral flake of unzoned pale green barian phlogopite (arrow) in olivine calciocarbonatite from Sukulu. Field of view is 3 mm across; crossed polars; sample BM–1990–P4(346). Numbers refer to compositional zones described in Fig. 6.

crystals of dolomite occur in the calciocarbonatite [P4(74)]. The calcite occurs as interlocking plates averaging 1 mm across. They have sutured margins and commonly show triple junctions. Magnetite forms small (<0.5 mm) scattered equant cubic crystals usually embedded in calcite. The apatite occurs in clusters of relatively large (2 mm) round to subprismatic crystals with abundant inclusions.

The phlogopite grains in calciocarbonatite [P4(46,73,75 and some in 45)] form zoned ragged plates 1–10 mm across (Fig. 1). The larger crystals have a core (X olive green, $Y = Z$ pale brown) that is strongly lobate, particularly along the cleavages. The abrupt and lobate nature of the core is taken to indicate resorption. The phlogopite overgrown around the core and in cracks and cleavages in the plates is brownish (X pale brown, $Y = Z$ orange-brown). At the rim, the orange-brown color becomes deeper, and the pleochroism is reversed. The mica is optically identical to what has been termed "tetraferriphlogopite" by other authors (*e.g.*, Gaspar & Wyllie 1987). Smaller crystals are commonly lath-shaped, have a pale brown center and are zoned to an orange-brown rim, even deeper in color than around the larger crystals. These rims also exhibit reverse pleochroism (Fig. 2).

The phlogopite crystals in calciocarbonatite sample [P4(74)], and a few in [P4(45)], are texturally different. They form large, unzoned pale green to pale yellow euhedral flakes up to 4 mm in length. Sample [P4(346)] contains magnetite, some subprismatic crystals of apatite, a few subhedral crystals of olivine (Fo_{88}) and euhedral flakes of phlogopite like those in [P4(74)]. The flakes are not zoned, are not deformed and have a clean, subhedral boundary against the enclosing crystals of calcite; this texture is interpreted to mean that the calcite and phlogopite crystallized in equilibrium. The pleochroism is X yellow-brown, $Y = Z$ green (Fig. 3).

Nooitgedacht, Transvaal

The sample of white calciocarbonatite taken from carbonatite [86CN9] at Nooitgedacht consists mainly of calcite with triple junctions, abundant oval prismatic apatite, lamellar-twinned subprismatic clinohumite, some euhedra of pyrochlore and two distinct textural types of phlogopite. The first forms clusters of small reversely zoned flakes associated with magnetite (Clarke *et al.* 1993). The second type forms isolated euhedral flakes that have a pale green-gray core (normal pleochroism) and colorless rim.

ANALYTICAL TECHNIQUES

Drill-core samples of carbonatites were chosen to ensure minimal secondary alteration due to weathering. Core material was obtained from the boreholes drilled by the Geological Survey of Uganda at Busumbu and Sukulu complexes. The cores are now stored at The Natural History Museum, London (formerly British Museum, Natural History) with numbers BM 1990, P4(1–129 and 346) for Sukulu samples and BM 1990,

TABLE 1A. ZONED PHLOGOPITE CRYSTAL, BUSUMBU

	Central flake	Near center	Towards edge	Near edge	Rim	Rim
stage*	1	2	3	3	4	4
SiO_2	38.44	41.31	40.42	40.29	39.88	38.59
TiO_2	1.26	0.36	0.46	0.47	1.44	1.43
Al_2O_3	13.07	10.86	10.68	10.46	11.09	11.13
FeO^T	13.56	9.37	10.96	14.48	14.90	14.65
MnO	0.28	0.26	0.20	0.24	0.20	0.11
MgO	17.35	21.66	20.86	18.36	16.66	16.73
CaO	0.04	0.04	0.02	0.09	0.16	0.26
Na_2O	0.64	0.55	0.56	0.61	0.57	0.35
K_2O	9.56	9.92	9.89	9.18	9.45	9.70
BaO	0.26	0.12	0.15	0.10	0.09	0.07
V_2O_3	0.03	bd	bd	bd	0.04	0.02
total	94.45	94.43	94.19	94.25	94.44	93.01
			cations to 22 oxygens			
Si	5.78	6.07	6.02	6.07	6.02	5.93
Ti	0.14	0.04	0.05	0.05	0.16	0.17
Al	2.32	1.88	1.87	1.86	1.97	2.02
Fe	1.71	1.14	1.36	1.82	1.88	1.88
Mn	0.03	0.03	0.03	0.03	0.03	0.02
Mg	3.89	4.74	4.63	4.12	3.74	3.83
Ca	0.00	0.00	0.00	0.02	0.03	0.04
Na	0.19	0.16	0.16	0.18	0.17	0.10
K	1.84	1.86	1.88	1.76	1.82	1.90
Ba	0.02	0.00	0.01	0.00	0.00	0.00
Fe/(Mg+Fe)	0.31	0.19	0.23	0.31	0.33	0.33

* Stage numbers correspond to those listed at the end of the contribution. bd: below detection. Compositions are reported in wt.%.

P5(1–60) for Busumbu samples. In the text and tables, these are referred to, for example, as P4(74) and P5(38).

Phlogopite compositions in the Uganda rocks (Tables 1, 2) were obtained from polished thin sections by wavelength-dispersion methods on the ARL–EMX–SM electron microprobe at the University of Iowa and the Cameca SX–50 electron microprobe at the University of Chicago. The standards, operating conditions and data-reduction technique used were the same as described by McCormick & Heathcote (1987); in addition, the concentration of Ba was determined. The analyses of the Transvaal phlogopite (Table 3) were made on the JEOL JXA–8600S microprobe at the University of Leicester, by wavelength dispersion as described by Clarke *et al.* (1993). Care was taken in both laboratories to avoid spurious high readings for Ti caused by the overlap of the Ti$K\alpha$ and Ba$L\beta$ lines.

Mineral Chemistry of Phlogopite

Stages of crystallization

Integrating the several zoned sequences described above, we conclude that the following seven stages of crystallization of micas can be correlated with

TABLE 1B. REPRESENTATIVE COMPOSITIONS OF ZONED PHLOGOPITE IN THE BUSUMBU BOREHOLE

no.	P5(38)				P5(37)		P5(39)		P5(36)			
stage	2	3	2	3	4	4	4	3a	3a	4a	3a	4a
pleochroism	GB/Oc	O/Or*	GB/Oc	O/Or	O/pO	O/pO	O/pO	OB/O	OB/Oc	OB/Or	GB/Oc	OB/Or
SiO_2	39.20	39.19	40.80	39.06	37.96	37.72	38.47	38.77	38.53	39.10	39.74	39.13
TiO_2	0.93	0.60	0.30	1.42	1.93	1.75	2.28	1.96	1.54	1.57	0.45	1.96
Al_2O_3	11.05	10.76	10.48	11.57	12.55	12.64	12.50	12.45	11.34	11.16	10.32	10.98
FeO^T	15.33	14.96	10.69	15.32	16.25	16.05	16.02	15.74	16.53	16.36	15.37	16.37
MnO	0.28	0.28	0.27	0.19	0.45	0.48	0.41	0.43	0.39	0.37	0.35	0.35
MgO	17.16	17.83	20.88	17.39	16.45	16.33	16.40	16.44	16.17	16.57	18.27	16.41
CaO	0.07	0.07	0.03	0.07	bd	bd	bd	bd	bd	0.25	0.04	0.20
Na_2O	0.54	0.58	0.63	0.38	0.44	0.44	0.50	0.43	0.62	0.51	0.51	0.52
K_2O	9.47	9.31	9.87	9.84	9.77	9.83	9.75	9.76	9.54	9.69	9.55	9.64
BaO	0.04	0.05	0.04	0.06	0.13	0.17	0.16	0.12	0.13	0.03	0.06	0.16
V_2O_3	bd	0.03	bd	0.05	0.04	0.04	0.06	bd	0.04	bd	bd	0.04
total	94.06	93.62	93.97	95.28	95.92	95.39	96.47	96.06	94.79	95.59	94.66	95.72
					cations to 22 oxygens							
Si	5.96	5.98	6.07	5.87	5.71	5.71	5.74	5.79	5.87	5.89	6.01	5.89
Ti	0.10	0.07	0.03	0.16	0.22	0.20	0.25	0.22	0.17	0.18	0.05	0.22
Al	1.98	1.93	1.83	2.04	2.22	2.25	2.20	2.19	2.03	1.98	1.84	1.95
Fe	1.95	1.91	1.33	1.93	2.05	2.03	2.00	1.97	2.11	2.06	1.94	2.06
Mn	0.03	0.04	0.03	0.02	0.06	0.06	0.05	0.05	0.05	0.05	0.05	0.05
Mg	3.89	4.05	4.63	3.90	3.69	3.68	3.65	3.66	3.67	3.72	4.12	3.68
Ca	0.01	0.01	0.00	0.01	0.00	0.00	0.00	0.00	0.00	0.04	0.00	0.03
Na	0.16	0.17	0.18	0.11	0.13	0.13	0.14	0.13	0.18	0.15	0.15	0.15
K	1.84	1.81	1.87	1.89	1.88	1.90	1.85	1.86	1.85	1.86	1.84	1.85
Ba	0.00	0.00	0.00	0.00	0.00	0.01	0.00	0.00	0.00	0.00	0.00	0.01
Fe/(Mg+Fe)	0.33	0.32	0.22	0.33	0.36	0.36	0.35	0.35	0.37	0.36	0.32	0.36

* Bold type: reverse pleochroism. Symbols: G: green, B: brown, O: orange, Y: yellow, p: pale, c: core, r: rim. Compositions are expressed in wt.%.

TABLE 2. REPRESENTATIVE COMPOSITIONS OF ZONED PHLOGOPITE IN THE SUKULU BOREHOLE

no.	P4(73)		P4(74)		P4(75)				P4(45)		P4(346)	
stage	2	3	6	7	2	3	4	4	3a	4a	6	7
pleochroism	G/YBc	pYO/Or	pG/pY	pG/pY	G/Oc	pY/Or	pO/O	pO/O	pGB/O	pOB/O	pG/pY	pG/pY
SiO_2	39.78	41.37	38.80	39.31	40.44	42.17	42.36	42.56	41.93	40.98	37.71	38.96
TiO_2	0.52	0.15	bd	0.03	0.83	0.10	0.12	0.07	bd	bd	0.27	0.09
Al_2O_3	12.90	11.16	14.56	14.19	13.09	10.73	9.91	9.78	11.78	12.08	17.56	15.63
FeO^T	5.94	4.50	2.35	2.35	6.10	5.20	5.88	6.02	2.72	2.30	5.48	2.98
MnO	0.04	0.04	0.04	0.05	0.08	bd	bd	bd	0.05	0.05	0.08	0.04
MgO	22.85	24.68	24.53	24.94	22.99	25.59	25.15	25.02	26.23	25.79	22.73	24.90
CaO	bd	0.06	bd	0.16	bd	0.07	0.06	bd	bd	0.06	bd	0.12
Na_2O	0.92	0.80	0.44	0.56	0.99	0.81	0.74	0.56	1.51	1.43	1.12	1.23
K_2O	8.90	9.31	9.66	9.43	9.37	9.88	9.75	9.98	8.29	8.16	8.61	7.93
BaO	0.32	0.06	1.38	1.13	0.28	bd	bd	0.12	0.25	0.49	1.75	2.47
V_2O_3	0.03	bd	bd	bd	bd	bd	bd	bd	bd	bd	0.04	bd
total	92.19	92.14	91.76	92.15	94.16	94.54	93.97	94.10	92.76	91.32	95.36	94.36
					cations to 22 oxygens							
Si	5.88	6.06	5.73	5.76	5.86	6.06	6.14	6.17	6.03	5.99	5.43	5.61
Ti	0.06	0.02	0.00	0.00	0.09	0.01	0.01	0.00	0.00	0.00	0.03	0.01
Al	2.24	1.93	2.53	2.45	2.24	1.82	1.69	1.67	2.00	2.08	2.98	2.65
Fe	0.73	0.55	0.29	0.29	0.74	0.62	0.71	0.73	0.33	0.28	0.66	0.36
Mn	0.00	0.00	0.00	0.00	0.00	0.00	0.00	0.00	0.00	0.00	0.01	0.00
Mg	5.03	5.39	5.40	5.45	4.97	5.48	5.43	5.40	5.62	5.61	4.88	5.35
Ca	0.00	0.01	0.00	0.03	0.00	0.01	0.01	0.00	0.00	0.00	0.00	0.02
Na	0.27	0.23	0.13	0.16	0.28	0.22	0.21	0.16	0.42	0.41	0.31	0.35
K	1.68	1.74	1.82	1.77	1.73	1.81	1.80	1.85	1.52	1.52	1.58	1.46
Ba	0.02	0.00	0.14	0.06	0.02	0.00	0.00	0.00	0.04	0.03	0.10	0.14
Fe/(Mg+Fe)	0.13	0.09	0.05	0.05	0.13	0.10	0.12	0.12	0.06	0.05	0.12	0.06

Compositions are expressed in wt.%.

sequences of fractional crystallization of carbonatite magma and of events during the assimilation of wall rocks. The availability of Al is the dominant factor controlling the formation of the various micas. The precise chemical composition of the micas, particularly the Fe/(Mg + Fe) ratio, varies from complex to complex, but it is the chemical trends exhibited by the micas that can be correlated. The terms "ferriphlogopite" and "ferribiotite" are used throughout the paper to indicate ferric-iron-bearing phlogopite and biotite. The trends are divided into stages, as follows, and these stage numbers are the numbers given in Figures 4–7: 1. Phlogopite crystallized in the earliest calciocarbonatite magma. 2. Phlogopite crystallizes with decreasing aluminum and with decreasing Fe/(Mg + Fe). 3. Phlogopite crystallizes with continued decreasing aluminum, but with increasing Fe/(Mg + Fe) compared to stage 2. 4. Further aluminum-poor "ferriphlogopite" crystallizes, but with increasing Fe/(Mg + Fe). It may reach the "ferribiotite" composition. 5. The "ferriphlogopite" and "ferribiotite" rims are resorbed. 6. High-aluminum phlogopite crystals form, in some cases as an overgrowth on the earlier mica. This generation of mica commonly contains in excess of 1 wt% barium. 7. High-aluminum barian phlogopite contains less aluminum and more barium than in stage 6.

Compositional trends

Representative compositions of phlogopite and biotite for Busumbu are presented in Table 1, those for Sukulu in Table 2 and those for Nooitgedacht in Table 3. Separate types of phlogopite are determined by their optical characteristics and proportion of Al *versus* Fe/(Mg + Fe) value. We found that the types of phlogopite are most easily differentiated using the parameter [8 – (Si + Al) × 10] for a structural formula where O = 22. Total silicon and aluminum from the analyses are used to calculate the parameter (Figs. 4–7). We presume that the difference [8 – (Si + Al)] corresponds to the proportion of ferric iron. Positive values indicate "ferriphlogopite" and "ferribiotite"; negative values indicate the presence of Al in both tetrahedral and octahedral sites. The sample size was much too small to obtain Fe^{3+}/Fe^{2+} by wet-chemical or Mössbauer analyses. The phlogopite compositions in the samples described in this paper contain levels of total iron as those of McCormick & Heathcote (1987) and Heathcote & McCormick (1989). Heathcote & McCormick (1989) reported that Mössbauer analyses performed by Darby Dyer on selected samples of "ferriphlogopite" yield the same amount of Fe^{3+} as the difference of [8 – (Si + Al)] of the same sample.

Relative ages of the various compositional types of phlogopite were established by the consistent sequences of zoning in individual crystals, by the presence of xenocrysts and by cross-cutting criteria. Examples of zoning and overgrowth sequences from individual grains are shown in Figures 4–7 by trend lines with arrows indicating the rimward direction.

Busumbu

The zoned phlogopite xenocryst [P5(38)] shown in Figure 4, exhibiting evidence of resorption and overgrowth, yields a complete history of crystallization of the Busumbu carbonatite. The core of the xenocryst [× in Fig. 4] is a parallelogram-shaped gray-green "ghost" crystal with green to brown-green normal pleochroism. The tetrahedral aluminum parameter is equal to –1, and the Fe/(Mg + Fe) is equal to 0.31 (Fig. 4). These values are similar to those for phenocrysts of primary phlogopite from Morrilton, Arkansas (McCormick & Heathcote 1987) and Potash Sulfur Springs, Arkansas (Heathcote 1987, Heathcote & McCormick 1989).

The central "ghost" core is overgrown by a pale orange-brown phlogopite with green-brown to orange normal pleochroism (+ in Fig. 4). The Fe/(Mg + Fe) value drops to 0.2, whereas the aluminum parameter increases to 0.5; this phlogopite is then a "ferriphlogopite", *i.e.*, it contains ferric iron in the tetrahedral site ("tetraferriphlogopite" of Rimskaya-Korsakova & Sokolova 1964). The composition of this overgrowth (● in Fig. 4) varies from the core value above to the rim of the zone where the aluminum parameter ranges from +1 to 0.6 and the Fe/(Mg + Fe) ratio ranges from 0.25 to 0.30.

The outer edge of zone [3] is ragged and contains numerous small grains of magnetite, indicating a period of resorption. The resorbed rim is overgrown by orange phlogopite (○ in Fig. 4) with orange to pale orange reversed pleochroism. The aluminum parameter ranges from 0.5 to 0, and the Fe/(Mg + Fe) value, from 3.2 to 3.4. The outermost rim of this zoned crystal is a "ferribiotite" (Fig. 4). The Fe/(Mg + Fe) ratio of the last-formed "ferriphlogopite"–"ferribiotite" is nearly the same as that of the central "ghost" crystal.

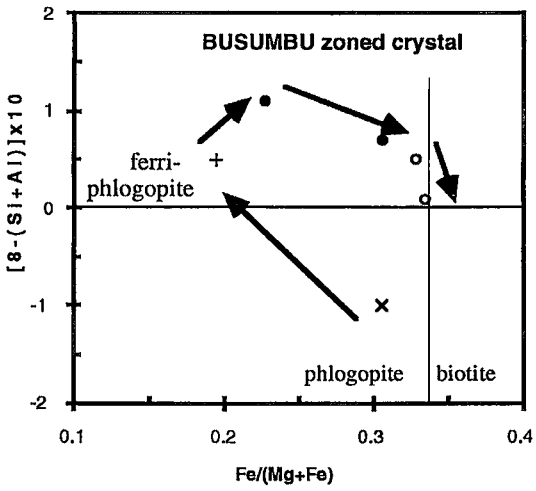

FIG. 4. Path of crystallization of the large zoned crystal of phlogopite shown in Fig. 1 [Busumbu, BM–1990–P5(38)]. The compositional zones are marked as in Fig. 2; × represents zone 1, +, zone 2, ●, zone 3, and ○, zone 4.

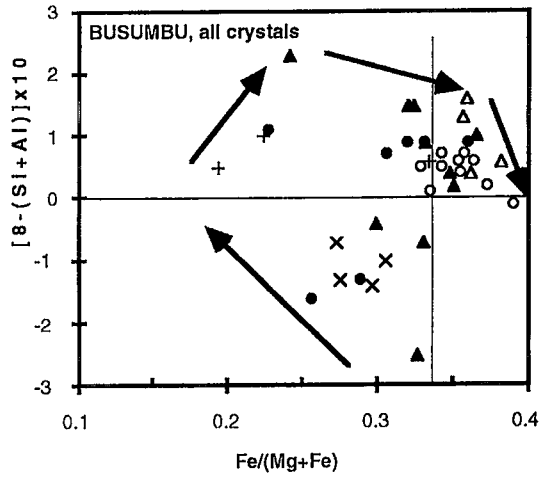

FIG. 5. Similar plot to Fig. 4, but for all 39 compositions determined from the Busumbu suite of calciocarbonatite, indicating overall trend of crystallization. The compositional zones are defined as in Fig. 4; in addition, ▲ represents zone 3a, and Δ, zone 4a.

Figure 5 shows the data for all the analyses taken from the six samples of carbonatite from Busumbu; representative compositions are found in Table 2. If comparison is made with Figure 4 and the zonal relations are taken into account, it can be recognized that the core of several crystals corresponds to the dark gray-green "ghost" crystal in Figure 4. The center of some other crystals, particularly the smaller ones, consists of "ferriphlogopite", and the margin of most of the crystals is "ferriphlogopite" grading into "ferribiotite", thus repeating and confirming the pattern seen in Figure 4.

Some of the mica compositions plotting as "ferriphlogopite" and "ferribiotite" in Figure 5 occur as small isolated crystals. These micas [▲ and Δ in Fig. 5] are taken to correspond with stages 3 and 4 in Figure 4 on the basis of their pleochroic colors and their position in Figure 5. Were it not for the few compositions plotted as stage 2, the data might suggest that the early phlogopite zoned directly toward the "ferribiotite" composition.

Sukulu

The compositions of phlogopite from the Sukulu carbonatite are all more magnesian than those of phlogopite from Busumbu, with only a little variation in the Fe/(Mg + Fe) value; however, they show a

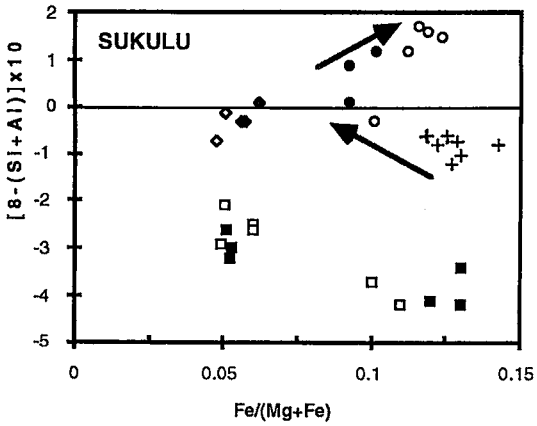

FIG. 6. Similar plot to Fig. 4 for Sukulu, showing (arrow) some similarity to the trend at Busumbu (Fig. 5). Zones 3a and 4a are from "clot-like" masses in P4(75) of rounded and zoned phlogopite crystals probably derived from xenolithic material. The two clusters 6 and 7 are the final-stage micas in samples from two adjacent boreholes (see Fig. 3). Compositional zones 2, 3 and 4 are defined as in Fig. 4; in addition, ♦ represents 3a, ◊, zone 4a, ■, zone 6, and □, zone 7.

similar trend of decreasing aluminum content in the tetrahedral site (Table 2, Fig. 6).

The center of the large deformed and resorbed flakes of phlogopite (+ in Fig. 6) exhibit normal pleochroism from green to greenish orange. The compositions of these grain centers plot in a group at Fe/(Mg + Fe) in the range 0.12 – 0.14, and the aluminum parameter ranges from –0.7 to –1.2. These consist of "ferriphlogopite" ("tetraferriphlogopite" of Rimskaya-Korsakova & Sokolova 1964).

The margin of these grains (3 in Fig. 6) exhibits normal pleochroism from deep to pale red-orange; the rim includes tiny iron oxide (magnetite ?) granules. The compositions of the margin form a trail in Figure 6; Fe/(Mg + Fe) decreases to 0.09 and then increases to 0.14, whereas the aluminum parameter increases from 0 to nearly 2 (Fig. 6).

A number of small, rounded crystals with brown-orange to cream-orange reverse pleochroism were analyzed (4 in Fig. 6). These micas are grouped at Fe/(Mg + Fe) in the range 0.11 to 0.13, nearly the same as that for zone 2, and have aluminum parameters ranging from 1 to 1.5. Aggregates of stubby, anhedral grains of mica are present in Sukulu sample P4(45). They are relatively Na-rich (*ca.* 1.5 wt% Na_2O) and are pleochroic from pale cream-green to a pale cream-rust color (3a in Fig. 6). These aggregates have a very narrow orange rim (4a in Fig. 6) and seem optically similar to the "ferriphlogopite" described above in zone 3. The above data suggest two separate sources for the crystallization of phlogopite prior to stage 4, which crystallized as reversed pleochroic "ferriphlogopite".

Phlogopite compositions of stages 6 and 7 of crystallization at Sukulu plot quite separately from those previously considered. They lie in the lower part of Figure 6 with [8 – (Si + Al)] × 10 equal to between –2 and –5. They are Al-rich and Ba-rich (1–3 wt% BaO, Table 2), unlike the mica at Busumbu, which has <0.5 wt% BaO. Such barian phlogopite is distinguished by its development as straight-edged and undeformed flakes, its pale green to cream pleochroic scheme, and its lack of an orange rim or border inclusions. There are two clusters of compositions on Figure 6, the less magnesian ones, mostly in sample P4(346), being very pale green and richer in Ti, Al and Na (up to 1.5 wt% Na_2O) than the more magnesian ones in sample P4(74).

The less magnesian variety of barian phlogopite is zoned, with the margin being richer in Na (with one exception), Si, Mg and Ba, and poorer in Al, Ti and Fe. The zoning in the more magnesian variety [in P4(74)] is negligible, but the composition of such phlogopite does lie in the direction of the zoned margin of the less magnesian variety, with higher levels of Si and Mg, lower levels of Al, Ti and Fe, but with less Na, and no difference in Ba concentration.

Nooitgedacht

The phlogopite of the Nooitgedacht calcio-carbonatite presents a simpler story. The minute flakes of reversely pleochroic "ferriphlogopite", which occur in between magnetite crystals, plot on a line almost coincident with the Sukulu "ferriphlogopite" trend (Fig. 7), but at lower Fe/(Mg + Fe) values. Compositions of the larger pale green-gray to colorless flakes in the Nooitgedacht sample plot as a chemically distinct group of aluminous barian phlogopite, which

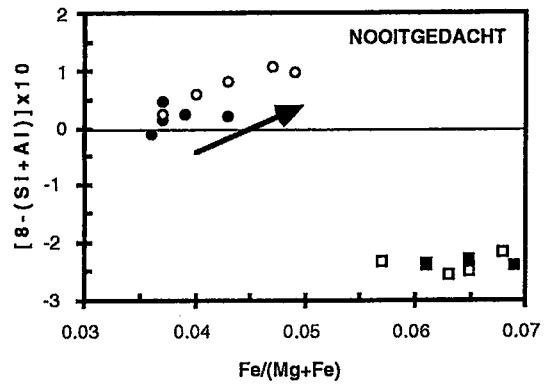

FIG. 7. Similar plot to Fig. 4 for Nooitgedacht, all in a single thin section. The compositional zones are defined as follows: ●, zone 3, ○, zone 4, ■, zone 6, and □, zone 7.

TABLE 3. COMPOSITION OF PHLOGOPITE FROM THE NOOITGEDACHT CALCIOCARBONATITE

	small flakes				big euhedral zoned flake			
stage	3	4	3	4	6	6	7	7
pleochroism	pO/Oc	pO/Or	pO/Oc	pO/Or	pG/pBc	pG/pBc	pY/pYr	pY/pYr
SiO_2	41.43	42.38	41.37	41.32	36.04	36.64	37.45	37.16
TiO_2	0.10	0.06	0.06	0.06	0.20	0.16	0.18	0.14
Al_2O_3	12.87	11.73	12.52	12.53	17.55	17.31	17.31	16.78
Cr_2O_3	bd	bd	bd	bd	0.04	bd	0.04	0.04
FeO^T	1.89	2.47	1.90	1.88	2.91	3.15	3.04	2.76
MnO	0.03	0.05	0.03	0.05	0.06	0.06	0.08	0.07
MgO	27.64	27.96	27.72	27.42	25.28	25.43	25.50	25.44
CaO	0.06	0.10	0.02	0.04	0.06	0.09	0.13	0.20
Na_2O	1.02	1.12	1.25	1.12	1.14	1.17	1.04	1.10
K_2O	9.19	9.40	8.96	9.18	7.41	7.64	8.16	7.95
BaO	1.05	0.22	1.07	0.88	5.19	4.17	3.41	3.16
F	0.55	0.44	0.37	0.45	0.70	0.46	0.46	0.62
Cl	bd	0.02	bd	bd	bd	bd	bd	bd
- O for F,Cl	(0.23)	(0.19)	(0.16)	(0.19)	(0.29)	(0.20)	(0.20)	(0.31)
total	95.60	95.76	95.11	94.74	96.29	96.08	96.60	95.11
	cations to 22 oxygens							
Si	5.85	5.95	5.86	5.88	5.23	5.29	5.35	5.37
Ti	0.01	0.01	0.01	0.01	0.02	0.02	0.02	0.02
Al	2.14	1.94	2.09	2.10	3.00	2.94	2.91	2.86
Cr	0.00	0.00	0.00	0.00	0.01	0.00	0.01	0.01
Fe	0.22	0.29	0.23	0.22	0.35	0.38	0.36	0.33
Mn	0.00	0.01	0.00	0.01	0.01	0.01	0.01	0.01
Mg	5.81	5.85	5.86	5.81	5.47	5.47	5.43	5.48
Ca	0.01	0.02	0.00	0.01	0.01	0.01	0.02	0.03
Na	0.28	0.31	0.34	0.31	0.32	0.33	0.29	0.31
K	1.65	1.68	1.62	1.67	1.37	1.41	1.49	1.47
Ba	0.06	0.01	0.06	0.05	0.30	0.24	0.19	0.18
F	0.25	0.20	0.17	0.20	0.32	0.21	0.21	0.28
Cl	0.00	0.01	0.00	0.00	0.00	0.00	0.00	0.00
Fe/ (Mg+Fe)	0.04	0.05	0.02	0.04	0.06	0.07	0.06	0.06

Compositions are reported in wt.%.

apparently is late in the crystallization of the calciocarbonatite; yet both groups (Al-poor and Al-rich phlogopites) occur within the same thin section. The compositions of barian phlogopite from Nooitgedacht (Table 3) occupy a comparable position to their more magnesian counterparts at Sukulu (Fig. 7), but with the difference that Ba and Al contents are both higher than at Sukulu.

Discussion of Factors Controlling the Crystallization of Mica in Carbonatite

The evidence presented above indicates that the composition of mica varies in response to changes in the carbonate magma while it crystallized and differentiated. This course of crystallization and differentiation is considered to have been affected by contamination and assimilation of wallrock material. A similar trend is present in carbonatites from Morrilton, Arkansas (McCormick & Heathcote 1987), Potash Sulfur Springs, Arkansas (Heathcote & McCormick 1989) and Nooitgedacht, Transvaal (Clarke *et al.* 1993, this paper).

The earliest-stage micas

In all cases studied, the earliest micas contain a small amount of aluminum in excess of that needed to fill the tetrahedral site. This conforms with previous observations (*e.g.*, Le Bas & Srivastava 1989) that the Al content of phlogopite crystallizing in carbonatite is low, *ca.* 12 wt% Al_2O_3 or less.

The Fe/(Mg + Fe) ratio of the earliest micas varies from complex to complex. Interpretation of textures and considerations of crystallization paths (Figs. 4–7) indicate that phlogopite phenocrysts with Fe/(Mg + Fe) approximately equal to 0.3, at Busumbu, are the earliest in the sequence of crystallization (Stage 1).

Differing Fe/(Mg + Fe) values of micas crystallizing in different bodies of calciocarbonatite depend on the composition of the host calciocarbonatitic magma and on the presence (or absence) of magnetite crystallizing from it. At Busumbu, Sukulu and the Arkansas complexes, the Fe/(Mg + Fe) value in the calciocarbonatite decreases initially, together with decreasing aluminum. The iron decrease in the mica seems to be correlated with the increasing oxygen fugacity in the carbonate magma, with consequent increase in the Fe^{3+}/Fe^{2+} ratio, building up to the precipitation of the magnetite seen at the rims of many grains of phlogopite (Stage 2). In other bodies of carbonatite, *e.g.*, Sukulu, the earliest micas present occur in aggregates of ragged crystals. These are considered to be xenocrysts from an earlier carbonatite or reaction product of an earlier carbonatite with wallrock.

Continued crystallization of phlogopite to "ferriphlogopite" (Stage 3) is marked by a change from decreasing to increasing $Fe_T/(Mg + Fe_T)$, impoverishment in aluminum, and a concomitant increase in Fe^{3+}. Even removing the calculated amount of Fe^{3+} from the "ferriphlogopite" compositions, the ratio $Fe^{2+}/(Mg + Fe^{2+})$ rises; this may be correlated with the increase in $Fe^{2+}/(Mg + Fe^{2+})$ of the magma (Stage 4).

The later-stage micas

There is an abrupt break in the crystallization path after the crystallization of the "ferriphlogopite"; this break is commonly marked by resorption of the reversed pleochroic rim of stage-4 phlogopite (Stage 5). The micas of stages 6 and 7 are Al-rich compared to those of stages 1–5; they also contain barium in excess of 1 wt%. The stage-6 mica is found as individual grains together with micas of stages 1–4 and as an overgrowth on micas of stages 1–4. The magma from which these stage-6 and -7 micas crystallized had to have been enriched in aluminum compared to the magma at stages 1–4.

Stage-6 and -7 micas have not been observed in the Busumbu carbonatites. At Sukulu, where later-stage Al-rich phlogopite is abundantly developed, xenoliths of pyroxenite or other mafic rocks are absent, but syenitic and fenitic xenoliths do occur. Such compositions would be more prone to dissolution in carbonatitic magma than would mafic xenoliths. Such

contaminant material would bring aluminum, silicon and alkalis to the carbonatite magma and would also bring about more rapid crystallization.

The high-Al phlogopite at Sukulu, Morrilton and Nooitgedacht resembles in Fe/(Mg + Fe) values the earlier "ferriphlogopite", indicating that the Fe–Mg relations were not altered by the assimilation, again suggesting that the material assimilated is felsic rather than mafic, unless of course the Fe/(Mg + Fe) ratio was the same in both host and contaminant. Such high-Al phlogopite (stage 6) also is rich in barium, a feature not seen in the earlier-stage micas. Barium in micas depends on the presence of additional aluminum in the tetrahedral site. All the cases of high-Al phlogopite studied here have BaO in excess of 1 wt%, and many with more than 2 wt%. It is uncertain whether the high barium content of the phlogopite is simply related to the high availability of aluminum in the carbonatite or whether it is related to later stages of crystallization of the carbonatitic magma, which is known to become Ba-rich by fractionation (Clarke *et al.* 1993), and to which crystallization of stage-6 phlogopite belongs. It is also possible that with potassium being lost to fenitization, barium, which is available, merely takes its place in the crystallizing mica.

Zoning from core to rim in the stage-6 high-Al phlogopite at Sukulu is marked by decreasing aluminum and Fe/(Mg + Fe), with barium remaining approximately constant (Stage 7).

Conclusions

Phlogopite compositions in carbonatite are chemically sensitive to the availability of Al, as well as the Mg/(Mg + Fe) value of the crystallizing carbonatitic magma. In contrast to the low Al contents of early-crystallizing phlogopite (commonly *ca.* 10 wt% Al_2O_3) in most examples of carbonatite, the high Al content of some later-crystallizing phlogopite (17 wt% Al_2O_3) indicates introduction of Al into the carbonatite magma, apparently as the result of incorporation and assimilation of wallrock material.

Acknowledgements

We are grateful to Mark Allen for guidance in the IBM and Mac formatting and plotting of these data using EXCEL 4, and thank The Natural History Museum, London for the loan of the samples analyzed. The reviews of André Lalonde and an anonymous referee led to numerous changes that greatly improved the presentation.

References

Baldock, J.W. (1967): *The Geology and Geochemistry of the Bukusu Carbonatite Complex, South-Eastern Uganda.* Ph.D. thesis, Univ. Leeds, Leeds, U.K.

_____ (1973): Potassic fenitization, trachytes and agglomerates at the Bukusu carbonatite complex. *Overseas Geol. Mineral Resources* **42**, 1-24.

Clarke, L.B., Le Bas, M.J. & Spiro, B. (1993): Rare earth, trace element and stable isotope fractionation of carbonatites at Kruidfontein, Transvaal, S. Africa. *In* Proc. 5th Kimberlite Conf., Vol 1. Kimberlite, Related Rocks and Mantle Xenoliths. CPRM, Brasilia, Brazil (236-251).

Davies, K.A. (1956): The geology of part of south-east Uganda. *Geol. Surv. Uganda, Mem.* **VIII**.

Gaspar, J.C. & Wyllie, P.J. (1987): The phlogopites from the Jacupiranga carbonatite intrusions. *Mineral. Petrol.* **36**, 121-134.

Heathcote, R.C. (1987): *Mica Compositions and Carbonatite Petrogenesis in the Potash Sulfur Springs Intrusive Complex, Garland County, Arkansas.* Ph.D. thesis, Univ. of Iowa, Iowa City, Iowa.

_____ & McCormick, G.R. (1989): Major-cation substitution in phlogopite and evolution of carbonatite in the Potash Sulfur Springs complex, Garland County, Arkansas. *Am. Mineral.* **74**, 132-140.

King, B.C., Le Bas, M.J. & Sutherland, D.S. (1972): The history of alkaline volcanoes and intrusive complexes of eastern Uganda and western Kenya. *J. Geol. Soc. London* **128**, 173-205.

Le Bas, M.J. & Srivastava, R.K. (1989): The mineralogy and geochemistry of the Mundwara carbonatite dikes, Sirohi District, Rajastan, India. *Neues Jahrb. Mineral., Abh.* **160**, 207-227.

McCormick, G.R. & Heathcote, R.C. (1987): Mineral chemistry and petrogenesis of carbonatite intrusions, Perry and Conway counties, Arkansas. *Am. Mineral.* **72**, 59-66.

Modreski, P.J. & Boettcher, A.L. (1973): Phase relationships of phlogopite in the system K_2O – MgO – CaO – Al_2O_3 – SiO_2 – H_2O to 35 kilobars: a better model for micas in the interior of the Earth. *Am. J. Sci.* **273**, 385-414.

Rimskaya-Korsakova, O.M. & Sokolova, E.P. (1964): Iron–magnesium micas with reversed absorption. *Zap. Vses. Mineral. Obshchest.* **93**, 411-423 (in Russ.).

Verwoerd, W.J. (1967): The carbonatites of South Africa and South West Africa. *Geol. Surv. S. Afr., Handbook* **6**.

Woolley, A.R. (1969): Some aspects of fenitization with particular reference to Chilwa Island and Kangankunde, Malawi. *Bull. Brit. Mus. (Nat. Hist.) Mineral.* **2**, 191-220.

Received September 27, 1994, revised manuscript accepted October 3, 1995.